

# AEM INVESTIGATION OF TETRAHEDRALLY COORDINATED $Ti^{4+}$ IN NICKEL-TITANATE SPINEL

IAN M. ANDERSON\*,†, JIM BENTLEY\*, AND C. BARRY CARTER†

\*Oak Ridge National Laboratory, Metals and Ceramics Division, P.O. Box 2008, M.S. 6376, Oak Ridge, TN 37831-6376; †University of Minnesota, Department of Chemical Engineering and Materials Science, 421 Washington Ave. S.E., Minneapolis, MN 55455-0132

## ABSTRACT

The stoichiometry and site distribution of metastable nickel-titanate spinel has been studied with AEM. The results of EDXS and EELS agree that the metastable spinel is nonstoichiometric and titanium-deficient relative to its hypothetical endmember composition, " $Ni_2TiO_4$ ". The titanium deficiency has been determined by EELS to be  $\Delta = 0.025 \pm 0.005$ . Channeling-enhanced microanalysis and ELNES studies indicate that the  $Ti^{4+}$  and  $Ni^{2+}$  cations are in tetrahedral and octahedral coordination, respectively, so that the metastable spinel has the normal cation distribution:  $Ti_{1-\Delta}[Ni_{2(1+\Delta)}]O_4$ . This result is consistent with neutron powder-diffraction studies and  $SiO_2$ -solubility measurements of similar equilibrated and quenched spinel-containing specimens. Metastable nickel-titanate spinel therefore contrasts with stable stoichiometric spinels which tend to the inverse cation distribution,  $Me[MeTi]O_4$ .

## INTRODUCTION

As the characteristic scale of the microstructures of engineering materials and devices approaches the nanometer level,<sup>1</sup> the characterization of these structures becomes increasingly challenging. Analytical electron microscopy (AEM) offers a variety of characterization techniques for the structural and chemical analysis of materials with nanometer-scale resolution.<sup>2</sup> Among chemical analysis techniques, X-ray microanalysis (or energy-dispersive X-ray spectrometry, EDXS) and electron energy loss spectroscopy (EELS) can be used to extract not only quantitative local compositions, but also local site distributions and elemental oxidation states.<sup>3,4</sup>

The spinel-structured phase in the system  $NiO-TiO_2$  is a model material for chemical analysis with the high spatial resolution of AEM. The equilibrium spinel phase,  $Ni_{2(1+x)}Ti_{1-x}O_4$ , exists only above  $1425^\circ C$  and with a large cation excess.<sup>5,6</sup> During quenching, the nonstoichiometric phase decomposes into a more stoichiometric spinel,  $Ni_{2(1+\Delta)}Ti_{1-\Delta}O_4$ , and a periclase-structured phase, of nominal composition  $NiO$ . The quenched-in metastable spinel always coexists with nanometer-scale periclase-structured inclusions.<sup>7</sup> The high spatial resolution of AEM is therefore necessary in order to characterize the metastable quenched-in spinel phase directly. Stable stoichiometric titanate spinels tend to the inverse cation distribution,  $Me_{(tet)}[MeTi]_{(oct)}O_4$ , with  $Me = Mg, Mn, Fe, Co$ , and  $Zn$ . Neutron powder diffraction<sup>8</sup> and  $SiO_2$ -solubility studies<sup>9</sup> indicate that in the metastable nickel-titanate spinel the  $Ti^{4+}$  cation is tetrahedrally coordinated; the site distribution is therefore apparently  $Ti_{1-\Delta}[Ni_{2(1+\Delta)}]O_4$ . However, these earlier studies did not have sufficient spatial resolution to isolate the spinel phase in the nanometer-scale microstructure nor did they provide spectroscopic analyses of the metastable spinel.

Tetrahedral coordination of  $Ti^{4+}$  in crystalline oxides is rare. Nickel-titanate spinel is the only known nearly close-packed oxide with the  $Ti^{4+}$  cation in tetrahedral coordination. A rare stable stoichiometric compound with tetrahedral  $Ti^{4+}$  is  $Ba_2TiO_4$ .<sup>10</sup> However, this latter compound is of lower symmetry than spinel and the four oxygen anions surrounding the  $Ti^{4+}$  cation do not form a regular tetrahedron.<sup>11</sup> Titanium can be made to coordinate tetrahedrally in amorphous oxides. The strong octahedral site preference of the  $Ti^{4+}$  cation is exploited technologically in the production of glass-ceramics<sup>12</sup> in which the cation, initially made to assume tetrahedral coordination as a network modifier in the glass, achieves octahedral coordination by precipitating in the form of  $TiO_2$  crystallites; these tiny crystals then serve as sites for the controlled nucleation and growth of the fine ceramic grains from the glass. A nearly close-packed crystalline oxide with tetrahedral  $Ti^{4+}$  may also exhibit novel properties that can be exploited technologically.

## EXPERIMENTAL PROCEDURE

Powders with the composition NiO-20wt.% TiO<sub>2</sub> were equilibrated in air at 1488°C for 142 h and quenched in water, as has been detailed elsewhere.<sup>6</sup> The quenched specimens were subsequently annealed in air at 1200°C for 30 minutes and air quenched. The loosely sintered specimens were embedded in epoxy<sup>13</sup> and then cut into 200 µm-thick slices with a low-speed diamond saw. Thin-foil specimens suitable for AEM investigation were prepared with standard mechanical techniques: embedded slices were cut into 3 mm disks with an ultrasonic drill; these disks were lapped to ~100 µm, dimpled to ~20 µm, and ion-milled to perforation. The final stage of ion-milling was performed at a relatively low energy (3 keV) and incident angle (12°). A thin coat of carbon was applied in order to mitigate charging effects.

The specimens were examined at ORNL with a Philips EM400T AEM equipped with a field-emission electron gun (FEG) and operated at 100 kV. X-ray microanalysis and EELS were performed with an EDAX 9100 energy-dispersive X-ray spectrometer and a Gatan 666 parallel-collection electron energy-loss spectrometer, respectively. The specimens were cooled to -130°C during spectrum acquisition using a Gatan double-tilt cooling holder. For X-ray microanalysis, the majority of the self-supporting disc specimen was masked by a gold washer with a 0.5 mm × 2.0 mm slot in order to minimize secondary excitation effects.

## RESULTS

Figure 1 shows EDX spectra characteristic of the three different phases composing the specimen. Spectra characteristic of the periclase-, spinel-, and corundum-structured phases, of nominal compositions NiO, Ni<sub>2</sub>TiO<sub>4</sub>, and NiTiO<sub>3</sub>, respectively, are shown in Fig. 1a-c. The spectrum of the periclase-structured phase, Fig. 1a, is also shown at 20× magnification in order to show the Ti K<sub>α</sub> peak. (The two other small peaks visible in this enlargement are the Ni K<sub>α</sub> escape peak and the Fe K<sub>α</sub> peak, the latter probably due to secondary excitation of the objective pole-piece.) The sum of the number of counts in the K<sub>α</sub> peaks of titanium and nickel exceeds 5×10<sup>5</sup> for all three spectra. The ratio of the intensities of the Ti K<sub>α</sub> to the Ni K<sub>α</sub> characteristic peaks in Fig. 1 are:

$$\left(\frac{N_{\text{Ti}}}{N_{\text{Ni}}}\right)_{(\text{per})} = 0.0050; \left(\frac{N_{\text{Ti}}}{N_{\text{Ni}}}\right)_{(\text{sp})} = 0.463; \left(\frac{N_{\text{Ti}}}{N_{\text{Ni}}}\right)_{(\text{cor})} = 1.055. \quad (1)$$

so that, in particular,

$$\left(\frac{N_{\text{Ti}}}{N_{\text{Ni}}}\right)_{(\text{cor})} / \left(\frac{N_{\text{Ti}}}{N_{\text{Ni}}}\right)_{(\text{sp})} = 2.28. \quad (2)$$

EEL spectra of the spinel- and corundum-structured phases are shown in Figure 2. These spectra were acquired with a detector dispersion of ~1 eV per channel and show the Ti L<sub>2,3</sub>, O K, and Ni L<sub>2,3</sub> edges after background subtraction. The two spectra are normalized such that the areas beneath their Ti edges are identical. The number of counts above the L-edges of the transition-metal ions were measured for two sets of spinel and corundum spectra with several different background-subtraction windows. In all spectra, the number of counts measured above the Ni L edges was ~5×10<sup>4</sup>; the number of counts above the Ti L edge exceeded 1×10<sup>5</sup>. Based on these measurements:

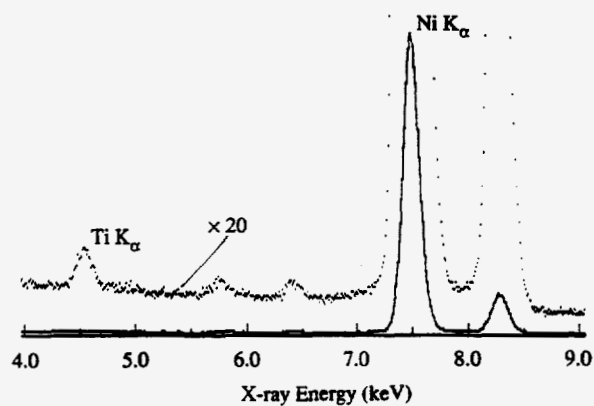
$$\left(\frac{N_{\text{Ti}}}{N_{\text{Ni}}}\right)_{(\text{cor})} / \left(\frac{N_{\text{Ti}}}{N_{\text{Ni}}}\right)_{(\text{sp})} = 2.10 \pm 0.02. \quad (3)$$

Figure 3 shows EDX spectra of the spinel-structured phases (a) Ni<sub>2(1+Δ)</sub>Ti<sub>1-Δ</sub>O<sub>4</sub> (NT) and (b) ZnNiTiO<sub>4</sub> (ZNT) with the specimens oriented for strong dynamical diffraction conditions at a {200} systematic row. Two spectra are superimposed in each part of the figure: (1) the shaded spectrum was recorded with the specimen oriented at the Laue (symmetric) orientation of the systematic row, whereas (2) the line spectrum (which appears black-on-white and white-on-black) was recorded near the Bragg orientation of the first-order allowed reflection, {400}, but with a positive excitation error. The relative sizes of the characteristic peaks in the spectra can be quantified with the ratio<sup>4</sup>  $R(X/Y) = (N_X^{(1)}/N_Y^{(1)}) / (N_X^{(2)}/N_Y^{(2)})$ , where  $N_X^{(n)}$  is the number of

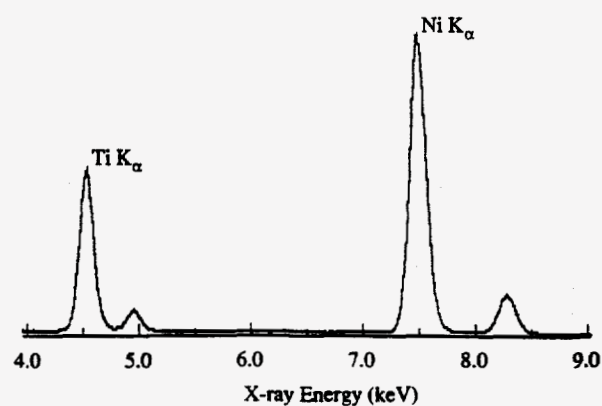
## **DISCLAIMER**

**Portions of this document may be illegible in electronic image products. Images are produced from the best available original document.**

1a



1b



1c

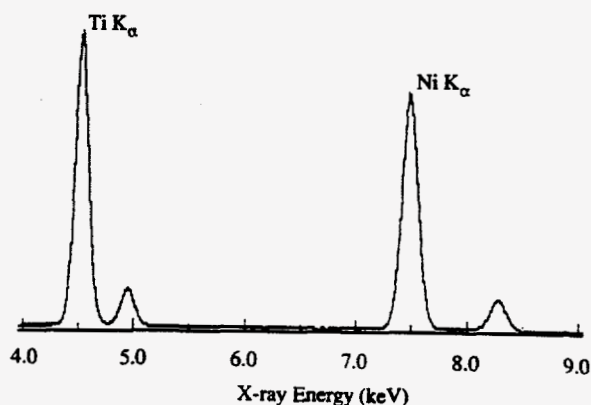


Figure 1.

X-ray microanalysis spectra of (a) periclase-, (b) spinel-, and (c) corundum-structured phases in the nickel-titanate specimen.

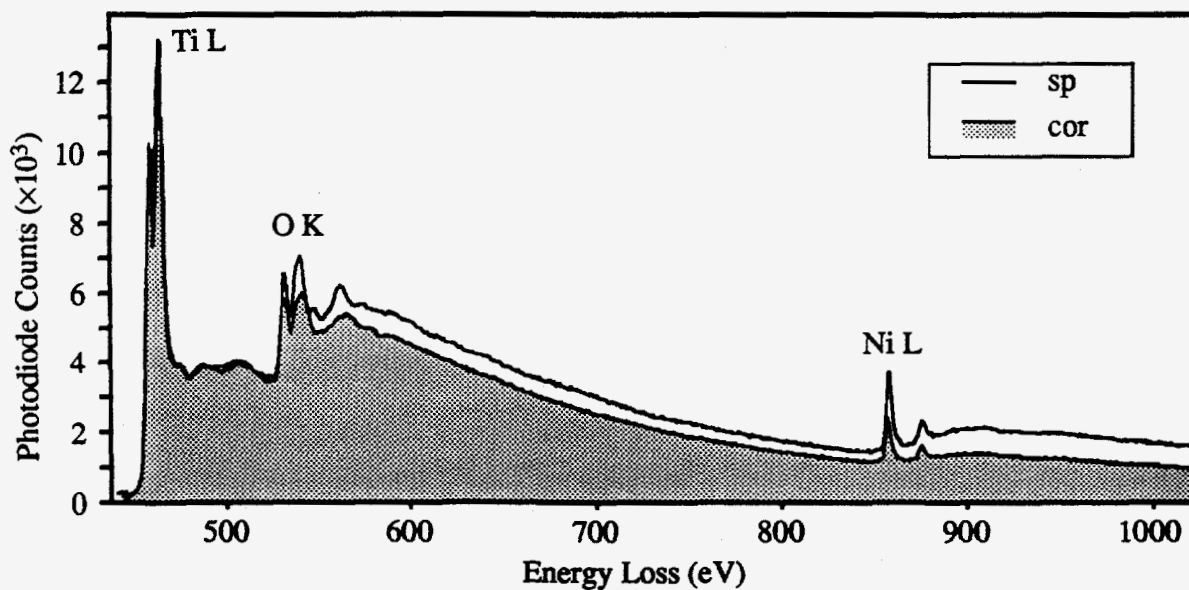
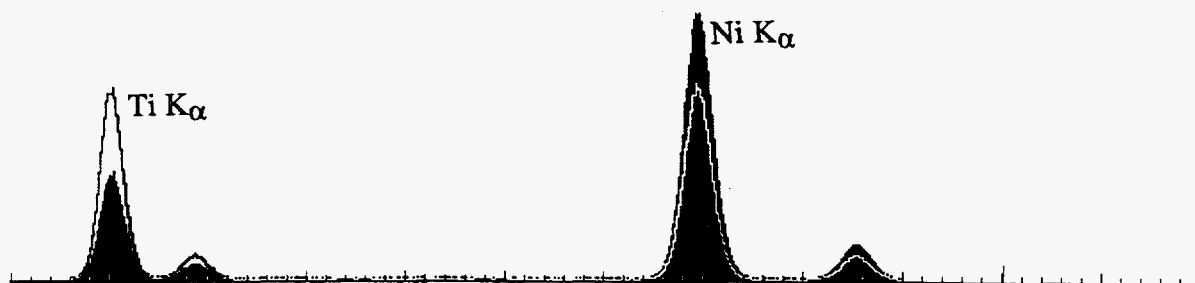


Figure 2. EEL spectra of the spinel- and corundum-structured phases. These spectra were acquired with a detector dispersion of  $\sim 1$  eV per channel and are shown after background subtraction. The scales of the two spectra were adjusted such that the areas beneath the Ti L edges are equal.

3a



3b

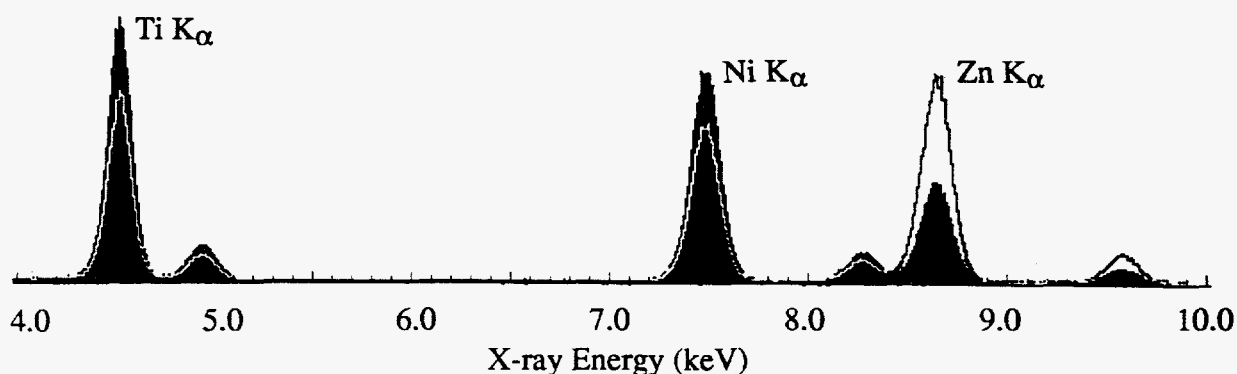
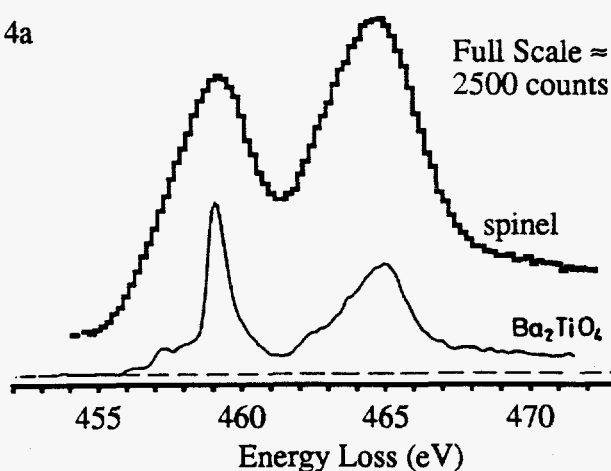


Figure 3. X-ray microanalysis spectra of (a) nickel-titanate spinel and (b) zinc-nickel-titanate-spinel, acquired under planar channeling conditions. The shaded spectra were acquired with the specimen at the Laue (symmetric) orientation; the superimposed line spectra were acquired with the specimen near the Bragg condition for the (400) reflection with a slightly positive excitation error.

4a



4b

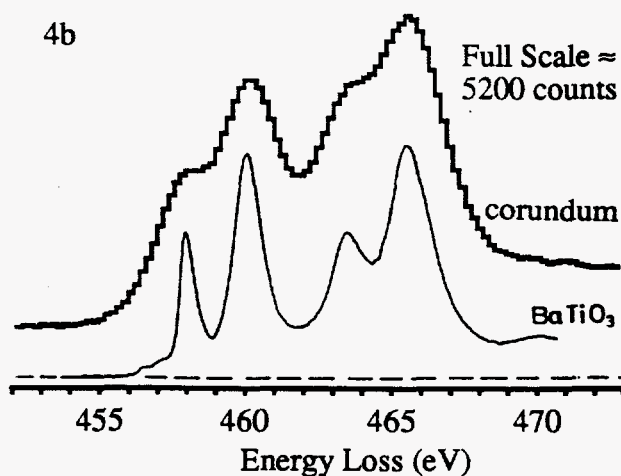


Figure 4. EEL spectra showing the near-edge fine structure of the Ti  $L_{2,3}$  edge of (a) the spinel- and (b) the corundum-structured phase. Inset are spectra reported by Brydson *et al.*<sup>14</sup> for (a)  $Ba_2TiO_4$  and (b)  $BaTiO_3$ , respectively.

counts recorded in the  $K_{\alpha}$  peak of element X in the  $n^{\text{th}}$  spectrum. Here,  $R_{\text{NT}}(\text{Ni/Ti}) = 2.50$ ,  $R_{\text{ZNT}}(\text{Ni/Ti}) = 0.97$ , and  $R_{\text{ZNT}}(\text{Ni/Zn}) = 2.79$ .

Figure 4 shows EEL spectra of the Ti  $L_{2,3}$  edge of the (a) spinel- and (b) corundum-structured phase, after background subtraction. These spectra were acquired with a detector dispersion of  $\sim 0.2$  eV per channel and show the near-edge fine structure (ELNES) of the Ti  $L_{2,3}$  edges for these two phases. Comparable spectra of Brydson *et al.*<sup>14</sup> for (a)  $\text{Ba}_2\text{TiO}_4$  and (b)  $\text{BaTiO}_3$  are inset.

## DISCUSSION

The ratios calculated in equations (2) and (3) should reflect the relative nickel to titanium concentrations in the spinel- and corundum-structured phases. X-ray microanalysis yields a value which is  $\sim 10\%$  higher than that yielded by EELS. The measured intensities of the characteristic peaks in the spectra shown in Fig. 1 are, however, expected to be representative of those excited in the primary excitation volume during analysis; corrections for absorption and secondary excitation effects should be modest. Since spectra are acquired in portions of the specimen such that only one phase is present through the thickness of the foil, the maximum thickness of the specimen should be  $\sim 100$  nm. Characteristic absorption lengths of Ni  $K_{\alpha}$  and Ti  $K_{\alpha}$  X rays in  $\text{NiO-20wt.}\% \text{TiO}_2$  are  $(\mu^{\text{Ni}})^{-1} \approx 97 \mu\text{m}$  and  $(\mu^{\text{Ti}})^{-1} \approx 39 \mu\text{m}$ . The absorption correction<sup>15</sup> for these two X-ray lines should therefore be  $\sim 0.15\%$ . The secondary fluorescence correction is quite modest for masked dimpled and ion-milled specimens,<sup>7,16</sup> even for strongly fluorescing specimens. Given that Ni  $K_{\alpha}$  fluoresce Ti  $K_{\alpha}$  X rays relatively weakly, the fluoresced intensity of Ti  $K_{\alpha}$  is expected to be  $\sim 0.1\%$  of the Ni  $K_{\alpha}$  intensity and therefore negligible. This expectation is supported by the spectrum of the periclase-structured phase (Fig. 1a): the measured Ti  $K_{\alpha}$  intensity is  $\sim 0.5\%$  of the Ni  $K_{\alpha}$  intensity; the contributions of *all* secondary excitation effects cannot exceed this value. It is possible that beam broadening may be responsible for the higher nickel-to-titanium ratio of the spinel for X-ray microanalysis; however, the intensity ratio of the characteristic peaks was found to be consistent among a number of spectra. Most likely, channeling effects are responsible for the higher nickel-to-titanium ratio in the spinel measured by X-ray microanalysis: as shown by Fig. 3a, a variation in the intensity ratio by a factor of 2.5 can be achieved under extreme diffraction conditions; a residual 10% effect is therefore conceivable and consistent with other studies.<sup>17</sup> EELS is less susceptible to the effects of channeling because those electrons which contribute to the effect tend to be scattered through angles larger than that subtended by the collection aperture.

Assuming that the corundum-structured phase is stoichiometric  $\text{NiTiO}_3$ , the nonstoichiometry of nickel-titanate spinel,  $\text{Ni}_{2(1+\Delta)}\text{Ti}_{1-\Delta}\text{O}_4$ , consistent with equation (3) is:

$$\Delta = 0.025 \pm 0.005, \quad (4)$$

a deficit of one of forty titanium cations (one in every fifth conventional unit cell) and with an average separation of  $\sim 14 \text{ \AA}$ . Residual nonstoichiometry in the spinel would be accommodated by point defects, which should introduce either diffuse reflections or superstructure reflections in the diffraction patterns of the spinel, neither of which are observed. However, the amount of diffuse scattering produced by a point defect concentration as dilute as that suggested by equation (4) may not be pronounced enough to be detected. If the corundum-structured phase is not stoichiometric, it would be expected to be NiO-rich; the value of  $\Delta$  would then be greater than 2.5%. However, any reasonable amount of nonstoichiometry falls well within the standard deviation in equation (4).

The values  $R_{\text{ZNT}}(\text{Ni/Ti}) = 0.97$  and  $R_{\text{ZNT}}(\text{Ni/Zn}) = 2.79$  show that the site distribution of zinc-nickel-titanate spinel is  $\text{Zn}[\text{NiTi}]\text{O}_4$ : an R-value near unity indicates a similar site distribution whereas a value far removed from unity indicates that the cations occupy different lattice sites.  $\text{ZnNiTiO}_4$  is a good standard for estimating the size of the channeling effect since  $\text{Zn}^{2+}$  has a strong tetrahedral site-preference whereas the  $\text{Ni}^{2+}$  and  $\text{Ti}^{4+}$  cations have strong octahedral site-preferences. The channeling-enhanced microanalysis of nickel-titanate spinel therefore strongly supports the normal cation distribution,  $\text{Ti}_{1-\Delta}[\text{Ni}_{2(1+\Delta)}]\text{O}_4$ , since  $R_{\text{NT}}(\text{Ni/Ti}) = 2.50$  is of the order of  $R_{\text{ZNT}}(\text{Ni/Zn})$ . The results of ELNES also substantiate the normal site distribution for metastable nickel-titanate spinel. The spectral features of the spinel- and corundum-structured phases in Fig. 4 are in good agreement with the superimposed spectra reported<sup>14</sup> for  $\text{Ba}_2\text{TiO}_4$  and  $\text{BaTiO}_3$ , which feature tetrahedrally and octahedrally coordinated  $\text{Ti}^{4+}$ , respectively.

## CONCLUSIONS

Metastable nickel-titanate spinel is characterized by the chemical formula,  $\text{Ti}_{1-\Delta}[\text{Ni}_{2(1+\Delta)}]\text{O}_4$ . The phase is titanium-deficient relative to its hypothetical endmember composition, " $\text{Ni}_2\text{TiO}_4$ ", and has the normal cation distribution. The degree of nonstoichiometry has been determined by EELS to be  $\Delta = 0.025 \pm 0.005$ . X-ray microanalysis, which yields a significantly larger nickel-to-titanium cation ratio in the spinel, was deemed less reliable than EELS. The probable reason for the inaccuracy is the large channeling effect for  $\text{Ti}_{1-\Delta}[\text{Ni}_{2(1+\Delta)}]\text{O}_4$ .

The high spatial resolution of the AEM was necessary to determine the stoichiometry and the site distribution of the spinel directly because of the nanometer-scale distribution of the periclase-structured NiO phase within the spinel. Larger regions of single-phase  $\text{Ni}_{2(1+\Delta)}\text{Ti}_{1-\Delta}\text{O}_4$  might be stabilized in thin-films deposited by a nonequilibrium technique such as sputtering or pulsed-laser deposition (PLD), which can be used<sup>18</sup> to deposit thermodynamically unstable phases given a suitable choice of substrate material. Thin films of  $\text{Ni}_{2(1+\Delta)}\text{Ti}_{1-\Delta}\text{O}_4$  might exhibit unusual properties given the unusual tetrahedral coordination of the  $\text{Ti}^{4+}$  cation in this compound.

## ACKNOWLEDGMENTS

This research was supported by the Division of Materials Sciences, U.S. Department of Energy, under contract DE-AC05-84OR21400 with Martin Marietta Energy Systems, Inc. and through the SHaRE Program under contract DE-AC05-76OR00033 with the Oak Ridge Institute of Science and Education; and by the National Science Foundation through grant number DMR-8901218. This research is also supported in part by an appointment to the Oak Ridge National Laboratory Postdoctoral Research Associates Program, which is administered jointly by the Oak Ridge Institute for Science and Education and Oak Ridge National Laboratory.

## REFERENCES

1. R. W. Siegel, *Annu. Rev. Mater. Sci.* **21**, 559-578 (1991).
2. *Principles of Analytical Electron Microscopy*, edited by D. C. Joy, A. D. Romig Jr., and J. I. Goldstein (Plenum Press, New York, 1986).
3. O. L. Krivanek, M. M. Disko, J. Taftø, and J. C. H. Spence, *Ultramicrosc.* **9**, 249-254 (1982).
4. J. C. H. Spence and J. Taftø, *J. Microsc.* **130**, 147-154 (1983).
5. W. Laqua, E. W. Schulz, and B. Reuter, *Z. anorgan. allg. Chem.* **433**, 167-180 (1977).
6. A. Muan, *J. Amer. Ceram. Soc.* **75**, 1357-1360 (1992).
7. I. M. Anderson, Ph. D. thesis, Cornell University, 1993.
8. G. A. Lager, T. Armbruster, F. K. Ross, F. J. Rotella, and J. D. Jorgensen, *J. Appl. Cryst.* **14**, 261-264 (1981).
9. N. F. Roberts and A. Muan, *J. Amer. Ceram. Soc.* **75**, 1382-1389 (1992).
10. P. Tarte, *Nature* **191**, 1002-1003 (1961).
11. J. A. Bland, *Acta Cryst.* **14**, 875-881 (1961).
12. W. D. Kingery, H. K. Bowen, and D. R. Uhlmann, *Introduction to Ceramics*, 2nd ed. (John Wiley and Sons, New York, 1976).
13. A. R. Spurr, *J. Ultrastr. Res.* **26**, 31-43 (1969).
14. R. Brydson, H. Sauer, and W. Engel, in *Transmission Electron Energy Loss Spectrometry in Materials Science*, edited by M. M. Disko, C. C. Ahn, and B. Fultz (The Minerals, Metals, and Materials Society, Warrendale, PA, 1992), pp. 131-154.
15. J. I. Goldstein, D. B. Williams, and G. Cliff, in reference (2), pp. 155-217.
16. I. M. Anderson, J. Bentley, and C. B. Carter, in preparation.
17. I. M. Anderson, in *Proceedings of the 50<sup>th</sup> Annual Meeting of the Electron Microscopy Society of America*, edited by G. W. Bailey, J. Bentley, and J. A. Small (San Francisco Press, San Francisco, CA, 1992), pp. 1240-1241.
18. I. M. Anderson, L. A. Tietz, and C. B. Carter, in *Structure and Properties of Interfaces in Materials*, edited by W. A. T. Clark, U. Dahmen, and C. L. Briant (Mater. Res. Soc. Proc. **238**, Pittsburgh, PA, 1992), pp. 807-814.

### **DISCLAIMER**

This report was prepared as an account of work sponsored by an agency of the United States Government. Neither the United States Government nor any agency thereof, nor any of their employees, makes any warranty, express or implied, or assumes any legal liability or responsibility for the accuracy, completeness, or usefulness of any information, apparatus, product, or process disclosed, or represents that its use would not infringe privately owned rights. Reference herein to any specific commercial product, process, or service by trade name, trademark, manufacturer, or otherwise does not necessarily constitute or imply its endorsement, recommendation, or favoring by the United States Government or any agency thereof. The views and opinions of authors expressed herein do not necessarily state or reflect those of the United States Government or any agency thereof.